Evaluation of Eelgrass Beds Mapping Using a High-Resolution Airborne Multispectral Scanner

Haiping Su, Duane Karna, Eric Fraim, Michael Fitzgerald, Rose Dominguez, Jeffrey S. Myers, Bruce Coffland, Lawrence R. Handley, and Thomas Mace

Abstract

Eelgrass (Zostera marina) can provide vital ecological functions in stabilizing sediments, influencing current dynamics, and contributing significant amounts of biomass to numerous food webs in coastal ecosystems. Mapping eelgrass beds is important for coastal water and nearshore estuarine monitoring, management, and planning. This study demonstrated the possible use of high spatial (approximately 5 m) and temporal (maximum low tide) resolution airborne multispectral scanner on mapping eelgrass beds in Northern Puget Sound, Washington. A combination of supervised and unsupervised classification approaches were performed on the multispectral scanner imagery. A normalized difference vegetation index (NDVI) derived from the red and near-infrared bands and ancillary spatial information, were used to extract and mask eelgrass beds and other submerged aquatic vegetation (SAV) in the study area. We evaluated the resulting thematic map (geocoded, classified image) against a conventional aerial photograph interpretation using 260 point locations randomly stratified over five defined classes from the thematic map. We achieved an overall accuracy of 92 percent with 0.92 Kappa Coefficient in the study area. This study demonstrates that the airborne multispectral scanner can be useful for mapping eelgrass beds in a local or regional scale, especially in regions for which optical remote sensing from space is constrained by climatic and tidal conditions.

Introduction

Eelgrass (*Zostera marina*), a submerged flowering plant that spreads by seed germination and rhizome growth, is found in nearshore estuarine and coastal water in the Northern Hemisphere at tidal elevations from +1.8 m (6 ft) to −6.7 m (22 ft) mean lower low water (MLLW). The dark green, long, narrow, ribbon shaped leaves of eelgrass plants with rounded tips can be 20 cm to 50 cm in length, with exceptional lengths up to about 2 m also observable (Tyler-Walter, 2004). A canopy height similar to the leaf lengths can be found depending on the intertidal locations, environments, and water column properties. Eelgrass may distribute in patches, fringe beds, or in large meadows that provide vital ecological functions ranging from substrate stabilization to providing a nursery and refuge for a high diversity of animals and plants (Phillips, 1972). The health status of eelgrass beds may also serve as a water quality indicator for coastal ecosystems (Dennison *et al.*, 1993). Given the high ecological importance of eelgrass beds and their reduction in distribution and abundance through shoreline development (Short and Burdick, 1996; Moore *et al.*, 1996), maintaining an inventory of this important resource is crucial to assessing and developing mitigation plans to offset future natural and unnatural losses.

Remote sensing has been used as a tool for mapping wetlands (e.g., National Wetlands Inventory Program) and coastal habitats (e.g., The National Oceanic and Atmospheric Administration's (NOAA) Coastal Change Analysis Program, or C-CAP) for decades. Guidelines were established in C-CAP to use various remotely sensed data, such as natural color and color infrared aerial photography and multispectral imagery, for developing estuarine habitat maps in coastal regions (Dobson *et al.*, 1999; Ferguson and Wood, 1990). Aerial photography has almost become the standard for most coastal wetland mapping (Ferguson and Wood, 1990; Ferguson *et al.*, 1993; Pasqualini *et al.*, 2001; Handley *et al.*, 2004), because it can provide detailed spatial resolution (sub-meter resolution) for intertidal and even shallow water vegetation interpretation with a relatively strong spectral response in the visible wavelengths. However, aerial photography is usually not radiometrically corrected, and it has limited spectral resolution. Therefore, it is difficult to use a digital image classification procedure to quantify the distribution and abundance of eelgrass beds from digitally scanned aerial photographs, partly because of limited spectral resolution and partly because of the need for nonlinear calibration of exposures between and within each photograph frame. Consequently, most aerial photography has been used for mapping eelgrass only through a manual photointerpretation process. However, an experienced wetland expert with aerial photointerpretation skills is required to provide acceptable results in the photointerpreta-

Haiping Su, Eric Fraim, Michael Fitzgerald, Rose Dominguez, Jeffrey S. Myers, and Bruce Coffland are with the University of California, Santa Cruz, NASA Ames Research Center, MS 240-6, Bldg 240, Room 219,Moffett Field, CA 94035 (hsu@mail.arc.nasa.gov).

Duane Karna was formerly with the U.S.-EPA Region 10 and has retired at 3822 183rd St. SW, Lynnwood, WA 98037.

Lawrence R. Handley is with the USGS-National Wetlands Research Center, 700 Cajundome Blvd., Lafayette, LA 70506.

Thomas Mace is with the NASA Dryden Flight Research Center, P.O. Box 273, MS-2516, Edwards, CA 93523.

Photogrammetric Engineering & Remote Sensing
Vol. 72, No. 7, July 2006, pp. 789–797.

0099-1112/06/7207–0789/$3.00/0

tion process. It can also be a time-consuming and labor-intensive process (Mumby *et al.*, 1999).

Recent advances in satellite technology have offered great potential for eelgrass mapping, particularly the successful launching of the Ikonos satellite in late-1999 and the QuickBird satellite in late-2001. These satellites carry multispectral sensors with high spatial resolution, ranging from a few meters to sub-meter. Unfortunately, acquisition of satellite images for submerged aquatic vegetation (SAV) mapping may not coincide with optimal conditions such as: (a) maximum low tide time window when the maximum area of vegetation is exposed to sunlight; (b) sediment brightness in the tidelands and under water where brighter background tends to have better delineation with SAV; and (c) water turbidity and depth where/when clearer and shallower water may produce more accurate results. Although the satellites (e.g., Ikonos) can be programmed at different view angles to increase the target acquisition opportunities, the time within maximum low tide window is still limited, especially in very cloudy coastal environments.

The medium spatial resolution satellite sensors, such as Landsat Themaptic Mapper (TM) and SPOT multispectral sensor (e.g., SPOT XS), may offer some opportunities for mapping the changes at a regional scales in coastal wetlands with a relatively longer term historical image database and cost-effective approach (Ferguson and Korfmacher, 1997; Mumby *et al.*, 1999; Mumby and Edwards, 2002). However, the medium spatial resolution (e.g., 30 m Landsat Thematic Mapper and 20 m SPOT High-Resolution Visible multispectral sensor) can hamper the actual use of the satellite images for mapping eelgrass beds or other SAV at a local scale if the eelgrass beds are in small patches (e.g., a few meters in diameter). In a recent study of detailed coral reef mapping, Lubin *et al.* (2001) used a coupled atmosphere-ocean discrete ordinates radiative transfer model to predict that satellite sensors, such as Landsat TM and Ikonos, may be adversely affected by the atmospheric Rayleigh scattering in the blue bands. Mumby and Edwards (2002) also demonstrated the weakness of satellite sensors (e.g., Landsat TM and Ikonos) over the airborne multispectral scanners (e.g., CASI) in their seagrass and coral reef mapping.

Given all the pros and cons of currently available satellite sensors and aerial photography, we hypothesized that airborne multispectral sensors may be used very efficiently for mapping eelgrass at a local and/or regional scales. Airborne multispectral sensors can offer adequate spectral and spatial resolution with optimum control and flexibility to select maximum low tide time windows and minimum cloud cover for image acquisition and digital classification, and may provide a cost-effective, time-saving and consistent approach for mapping a relatively large area compared to conventional aerial photointepretation (Mumby *et al.*, 1999; Mumby and Edwards, 2002).

A few studies carried out in the Pacific Northwest have been conducted to validate the airborne multispectral sensors approach. In Tillamook Bay, Oregon, Strittholt and Frost (1996) used a 1 m resolution and three-band multispectral airborne imaging system to determine abundance and distribution of eelgrass. Their overall 80 percent accuracy for a digital image classification method with field verification indicated that airborne multispectral imagery may be a cost-effective approach for mapping eelgrass habitats. In a similar study, Ritter and Lanzer (1997) used a more advanced multispectral airborne sensor, the Compact Airborne Spectrographic Imager (CASI), to map nearshore vegetation in Washington State's Puget Sound. The CASI system in this study was configured in 11 bands ranging from visible to near-infrared spectral wavelengths with a 4 m spatial resolution. A classification accuracy assessment was performed using 164 field points of data to verify a classified image map derived from the CASI interpretation. Based on their confusion matrix analysis, producer (a measure of possibility of a class labeled into the same class as it appeared in the field) and user (a measure of possibility of a class labeled into the same class as it determined in the image classification process) accuracies for eelgrass class were 81.7 percent and 90.5 percent, respectively. A series of digital geographic information system (GIS) vector layers with various scales also was created in this project and served as important baseline information for coastal resources managers and decision-makers. More studies of seagrass mapping using high-resolution multispectral scanners were conducted in different parts of the coastal regions, such as in the tropical Western Atlantic (Mumby *et al.*, 1997), over the Roscoff coastal zone of Brittany, France (Bajjouk *et al.*, 1996; Bajjouk *et al.*, 1998), and in the Turks and Caicos Islands of British West Indies (Mumby and Edwards, 2002). The results of these studies seem to suggest that the multispectral scanners are superior in overall accuracy and spectral and spatial resolution compared to the satellite sensors (e.g., Landsat TM, SPOT XS, and Ikonos).

Given the capabilities and flexibility of airborne multispectral sensors, this study was intended to further demonstrate that an airborne multispectral scanner with 12 relatively broad bands ranging from visible, near-infrared and mid-infrared to thermal wavelengths at a 5 m spatial resolution, may offer efficiencies in mapping eelgrass beds and delineating coastal wetlands at a local scale, as well as providing comparable accuracies to traditional airphoto interpretation. Therefore, this investigation evaluated a multi-step eelgrass image classification of airborne multispectral scanner data collected over part of the Northern Puget Sound, Washington, using a conventional airphoto interpretation.

Methods

Airborne Image Acquisition and Data Preparation

We conducted this study in the Northern Puget Sound of the Swinomish Indian Tribal Community (SITC) reservation (48° 24′ N, 122° 33′ W), about 80 km north of Seattle, Washington (Figure 1). There are approximately 650 hectares

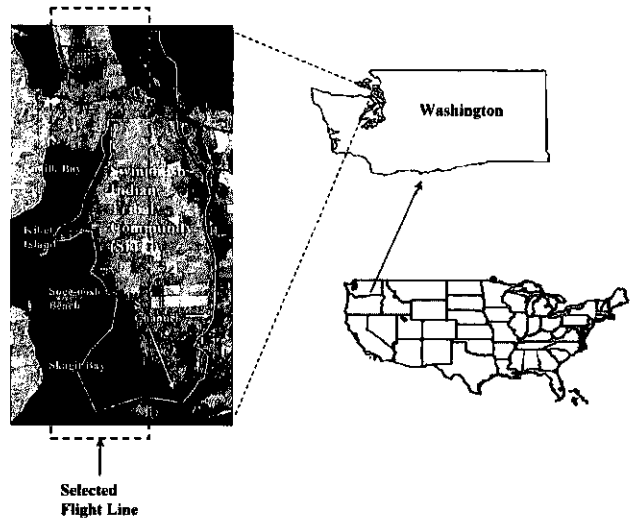

Figure 1. Study area on the west side of the Swinomish Indian Tribal Community (SITC) reservation.

of tidelands within the study area, about 90 percent of all tidelands on the SITC reservation.

This project was part of a joint U.S. National Aeronautics and Space Administration (NASA) - U.S. Environmental Protection Agency (EPA) effort to use advanced monitoring technology to protect the environment. A Daedalus 1268 multispectral scanner available from the Airborne Sensor Facility of the NASA Ames Research Center (Moffet Field, California) was used for this study. (Traditionally, this scanner is called the Airborne Thematic Mapper Simulator, as the Landsat TM bands can be synthesized from the higher resolution airborne data.) The 12 band sensor can be mounted either in a low altitude (flying at about 1.8 km altitude, such as KingAir Beechcraft B200 or Cessna Citation) aircraft to acquire multispectral scanner images at high spatial resolution (approximately 5 m) or in a high altitude (flying at about 20 km altitude, such as ER-2) aircraft to acquire medium (approximately 25 m) spatial resolution images. Total field of view from the sensor is 42.5 degrees. The 12 spectral bands cover a spectral range from visible, near-infrared and mid-infrared to thermal wavelengths. Bands 2, 3, 5, 7, 9, 10, and 11 (or 12) of the scanner have the same band wavelength as Landsat 4 or 5 Thematic Mapper bands 1, 2, 3, 4, 5, 7, and 6 (thermal) (Table 1). Additionally, four more bands in the sensor can provide more spectral information than the Landsat Thematic Mapper.

The airborne multispectral scanner data were acquired on 30 July 2000 during a near maximum low tide time window (about −0.9 m MLLW) over an altitude of 1.8 km at a nadir pixel size of 5 m. This timing was selected to maximize the amount of SAV that would be exposed without water cover and to minimize water depth over the remaining beds. A total of four flight lines in a north and south direction covered the intertidal and upland areas of the SITC reservation. A Wild RC-10 camera also was mounted in the airplane to acquire high spatial resolution color infrared (CIR) aerial photographs. Both the airborne scanner imagery and CIR photography were acquired under cloud-free conditions with a few areas of sun glint over the southern part of the study area visible in the CIR photography. Post-flight calibration was carried out with all in-flight recorded calibration parameters. The airborne multispectral scanner image data sets for all flight lines were in excellent condition.

In preparing the georeferenced base map, the CIR photographs were digitally scanned, and a professional photogrammetric engineering company created 1-foot spatial resolution Digital Orthophoto Quads (DOQ) to cover most of the SITC reservation. The horizontal and vertical accuracies of the DOQ were evaluated at ±1.5 m (±5 ft) and ±0.6 m (±2 ft) RMSE, respectively. All DOQ frames (created in the Washington State Plane projection coordinate system) were re-projected and re-sampled into the Universal Transverse Mercator (UTM) projection coordinate system with a 2 m spatial resolution. Finally, all DOQ frames were mosaicked together to create a DOQ base map layer for georeferencing the airborne scanner images acquired simultaneously.

TABLE 1. A LIST OF WAVELENGTHS FOR THE AIRBORNE MULTISPECTRAL SCANNER

Band	Wavelength (μm)	Compared to Landsat TM	Wavelength Description
1	0.42–0.45		Visible
2	0.45–0.52	TM1	Visible
3	0.52–0.60	TM2	Visible
4	0.60–0.62		Visible
5	0.63–0.69	TM3	Visible
6	0.69–0.75		Visible-Near infrared
7	0.76–0.90	TM4	Near infrared
8	0.91–1.05		Near infrared
9	1.55–1.75	TM5	Near infrared
10	2.08–2.35	TM7	Mid infrared
11 (High Gain)	8.5–14.0	TM6	Thermal
12 (Low Gain)	8.5–14.0	TM6	Thermal

Field Survey

In the month prior to the 30 July 2000 aerial mapping by NASA, field teams made up of personnel from the EPA Region 10 and from the Swinomish Indian Tribal Community established 11 ground control points from intertidal areas to the uplands in the study area. The control points were subsequently used to orthorectify the aerial photographs. In addition, the field teams also set up 21 SAV baseline stations, where composition and density of SAV were recorded and used to field verify interpretation and classification of the aerial photographs and airborne scanner imagery, respectively.

The control point markers in intertidal or wetland areas were made of 0.8 m (30 inches) wide white butcher paper fixed to the substrate, and those on the uplands were located on blacktop pavements and painted white. The control point markers were either "X" or "L" shaped, the letters were at least 3 m (10 feet) long and each stripe was at least 0.6 m (2 feet) wide. A hand-held Trimble GeoExplorer® Global Positioning System (GPS) unit was used to record locations for the center of the "Xs" and the junction of the two legs of the "Ls". The recorded GPS files were post-processed using differential corrections to control the accuracy within ±3 m.

The composition and density of SAV beds were measured in 0.25 m^2 quadrats at the 21 baseline stations. Each 0.25 m^2 quadrat was divided by monofilament into 25 subunits measuring 10 cm × 10 cm. The field teams recorded the distribution and abundance of eelgrass (*Zostera marina* and *Zostera japonica*) and other SAV (*Ulva* spp., *Fucus* spp., *Enteromorpha* spp., and several unidentified species of red and brown algae) using point-intercept frequencies of occurrence (Young *et al.*, 1998). Field personnel also sketched and photographed the eelgrass beds at each baseline station for additional information about eelgrass density measurement and its spatial extent of eelgrass nearby. This information was used to help photointerpretation and training pixel selection later. Plate 1 shows an example of an eelgrass density photograph taken over a 0.25 m^2 quadrat for station M3.

The GPS position of the center of the eelgrass baseline station was also recorded and differentially corrected. The results of this part of the survey can be found in Table 2. The eelgrass beds were designated as north (N), middle (M), southwest (SW), or east (E), indicating their locations in the study area. The north beds surveyed were north of Kiket Island on the east side of Similk Bay, the middle beds extended south side of Kiket Island to Snee-Oosh Beach, the southwest and largest beds were southwest of Snee-Oosh Beach and north of the southern end of the Swinomish Channel, and the east beds were located in the Swinomish Channel (Plate 2).

Image Processing and Analysis

To demonstrate and evaluate the procedure, one flight line covering more than 90 percent of the SAV in the study area was selected for the image analysis and processing. Ten of the 12 bands (excluding the two thermal bands) were used in the image classification.

A simple tangential distortion correction algorithm was used to reposition each pixel along the scanline. The off-nadir pixels in each scanline were re-sampled based on the scanner's view angles between two adjacent pixels using a nearest neighbor approach to preserve the spectral response of each scanline. However, the geometric distortion caused by the

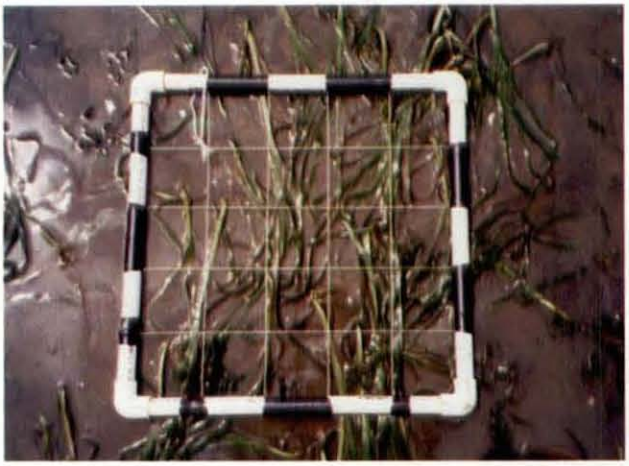

Plate 1. An example of eelgrass density measurement photograph taken at station number 3 in the middle section of eelgrass beds (M3) in the study area.

TABLE 2. EELGRASS COVERAGE MEASURED IN BASELINE STATIONS

Bay Segment Location	Station ID	Distance to Upland Edge of Bed (feet)	Eelgrass (%)	Other Plants (%)	Bare Substrate (%)
North	N1	24	92[1]	4	4
	N2	43	68	0	32
	N3	10	88	12	0
	N4	155	56	0	44
	N5	14	80	0	20
	N6	63	60	0	40
	N7	11	60	28	12
Middle	M1	17	60	0	40
	M2	17	76	0	24
	M3	111	48	0	52
	M4	74	24	60	16
	M5	14	28	72	0
Southwest	SW1	200	68	0	32
	SW2	42	96	4	0
	SW3	NM[2]	76	0	24
	SW4	80	52	0	48
East[3]	E1	10	68	0	32
	E2	24	72	8	20
	E3	9	84	0	16
	E6	NM	88	0	12
	E7	NM	60	20	20

Notes: [1]*Zostera japonica*; [2]not measured; [3]stations E4-E5 were small patches that were incompletely surveyed.

Plate 2. Location of the baseline stations overlaid on the digital ortho-photo quads (DOQ).

airplane motion (roll, yaw, and pitch) and one-dimensional relief displacement was not geometrically corrected in the simple tangential distortion correction process.

Because of the relatively stable flight conditions during the image acquisition and small topographic variation (approximately 3 to 5 m relief in the intertidal areas) of the study area, we used a non-parametric georeferencing approach. However, a first-order polynomial function for georeferencing the entire flight line could not achieve the spatial accuracy required for this study. Instead, we minimized the geometric effects with a stepwise 2-degree polynomial approach. First, we identified a total of 157 ground control points within the selected airborne scanner flight line and the DOQ base map layer through image matching. Then, we subdivided the entire flight line covering the study area into four segments with about 1,000 scanlines each. We built a 2-degree polynomial function for each segment and individually warped the scanner images into the DOQ base map coordinate system (UTM, WGS84, Zone 12) with a 5 m spatial resolution. Finally, we mosaicked all four segments of the warped images together to cover the study area. Errors for each segment image were controlled within ±5 m or about one pixel RMSE of the warped segment images.

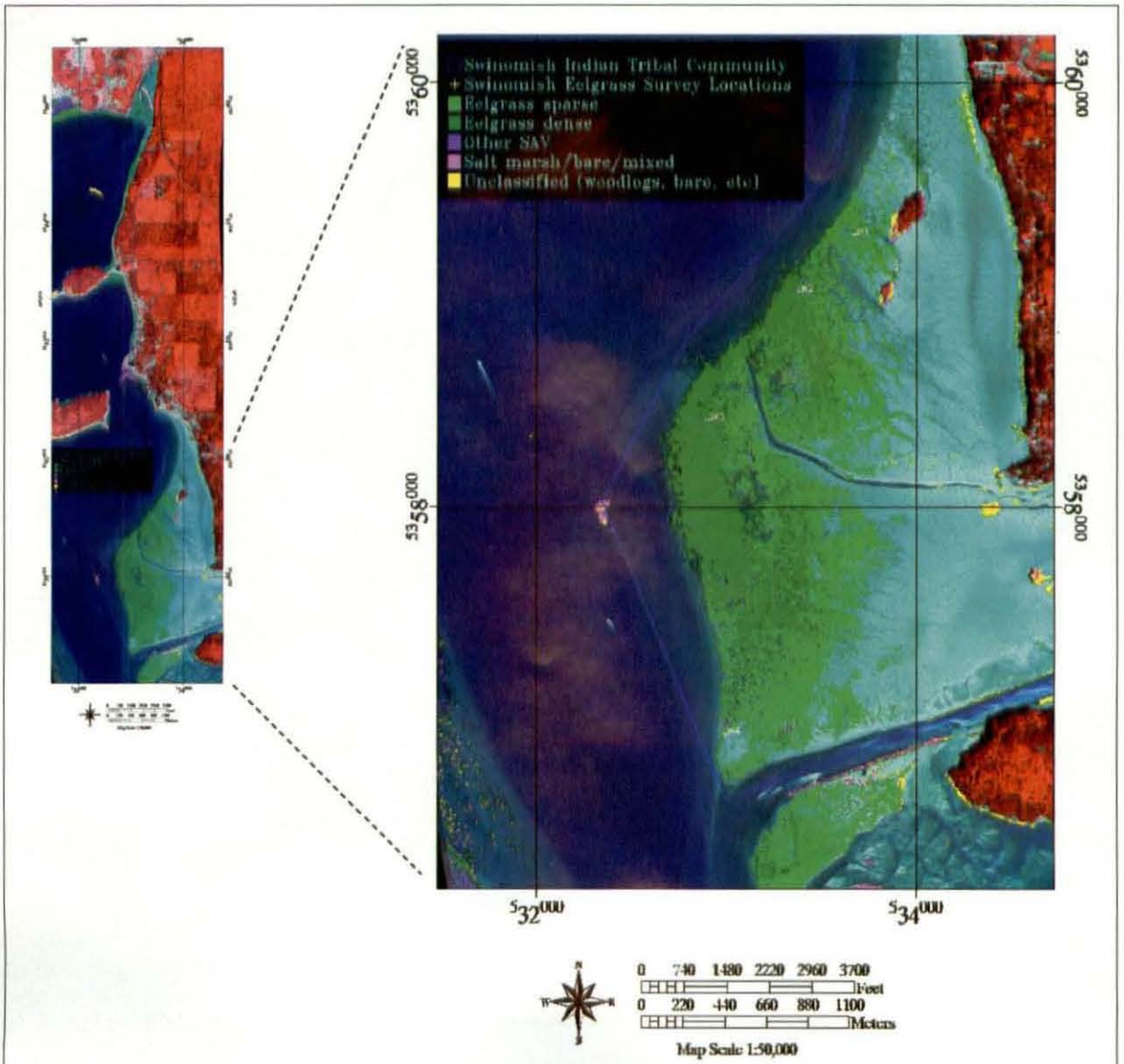

Plate 3. The study area eelgrass classification result overlaid on the false color composites of airborne multispectral scanner image and a zoom-in classification map for details.

Delineating eelgrass beds in intertidal areas is an extremely complicated process because spectral signals of uplands (or non-tidal wetlands), water columns, sediments, rocks, algae, and other submerged aquatic vegetation types intend to mix and/or intersperse with spectral signal of eelgrass beds within an imagery. For example, eelgrass can be detected in shallow water with a light sediment background better than in deeper water with a dark sediment background. In addition, the spatial resolution of the image can play an important part in eelgrass bed delineation because of patchy/sparse distribution and variable abundance (density) of eelgrass beds. How ever, it should be noted that the pixel spatial resolution of the airborne multispectral scanner depends upon the flight altitude and is adjustable.

In order to delineate the spectral variation in the intertidal areas, we elected to use a "double elimination" stepwise approach and consider one distinct spectral class at a time to extract eelgrass beds and other classes. The first step in this "double elimination" approach was to examine the spectral responses present in the entire flight line and the field survey information to define the number of classes that could be identified at the 5-meter spatial scale. Using an unsupervised classification (ISODATA method) for the entire flight line, we determined that some targets in the uplands and in the intertidal lands were spectrally similar in the multispectral scanner data. For example, the dark (shaded) forest areas in the uplands were confused with the dark signature of the eelgrass beds in the shallow water. Once we noticed these differences, we decided to mask the upland areas from the eelgrass beds classification. The intertidal areas and the water areas were defined by digitizing a polygon (area of interest) on the airborne image, thus eliminating the uplands. In some cases, salt marsh also was confused with the upland vegetation. However, use of contrast stretched multispectral imagery and high spatial resolution CIR aerial photography allowed us visually separate salt marsh areas from the uplands.

After masking out the upland areas, the unsupervised classification (ISODATA method) was reapplied to the intertidal and water areas of the image to identify 25 classes. Our wetland expert and field survey personnel carefully

TABLE 3. DEFINED MAPPING CLASSES FOR THE STUDY AREA

Class	Description
Eelgrass dense	More than 60% eelgrass beds cover in continuous distribution patterns
Eelgrass sparse	About 20–60% eelgrass beds cover in discontinuous distribution patterns or patches
Other SAV	More than 60% other submerged aquatic vegetation cover or without eelgrass present
Bare earth	Bare rocks, cobbles, beach, or mud flats
Salt marsh	Estuarine emergent wetlands

examined the classification map and the field survey information. Finally, with this preliminary process, we were able to roughly label five classes from the 25 ISODATA classes in the intertidal areas at the 5-meter resolution (Table 3).

The second step in the "double elimination" approach was to eliminate water areas where seagrass and other SAV were no longer detectable by the airborne sensor during the time of image acquisition. We used an unsupervised classification method to define the boundary between the intertidal and the water areas. We also used a normalized difference vegetation index (NDVI) image derived from near-infrared and red bands to identify areas of SAV in the deeper water. These boundaries marked the intertidal regions for further image processing.

The third step was to mask out the "bare earth" class where no SAV were detectable. We used the NDVI image again to extract the "bare earth" class from the image. Therefore, the only classes requiring image classification procedures were the eelgrass (sparse and dense), other SAV, and salt marsh classes as defined in Table 3.

The fourth step was to develop the training classes from field baseline survey information. Because of the limited spatial extent of each baseline station (0.25 m^2 quadrat each), we had to locate the pixels in and nearby each selected baseline station with the field photographs and sketches from the baseline stations using image analysis software. From these areas of the image, a sufficient sample size (at least 35 pixels) was extracted for each training class using the pixel region growth tool in the image analysis software. Training pixels for each class also were verified in the DOQ aerial photographs (1-foot resolution) with photointerpretation.

The fifth step was to evaluate the spectral separability of training classes. Each training class pair was controlled at a maximum separability value from 1.8 to 2.0, using the Jeffries-Matusita transformed divergence measure (Jensen, 1986). Using the separability of the training classes as a measure of uniqueness, we maximized the statistical differences between training sets in the classification stage.

The sixth step was to perform a supervised classification with a maximum likelihood classifier for the study area with the classes listed in Table 3, except "bare earth." The seventh and final step was to refine the classified image by adjusting classification rule images using different thresholds, especially for dense and sparse eelgrass classes. The finalized classification was combined with the "bare earth" class. A total of 2.8 percent of the pixels were unclassified, most of which were in small patches identified as wood debris, logs, tree shadows, or other SAV mixed with salt marsh close to the upland edge within the wetland boundary. Therefore, we assigned the unclassified pixels into a "salt marsh/mixed" class in the final classification image. Plate 3 shows all classes overlaid (except "bare earth") on the false color composite of the airborne scanner image. We summarized the "double-elimination" stepwise approach in a flowchart shown in Figure 2.

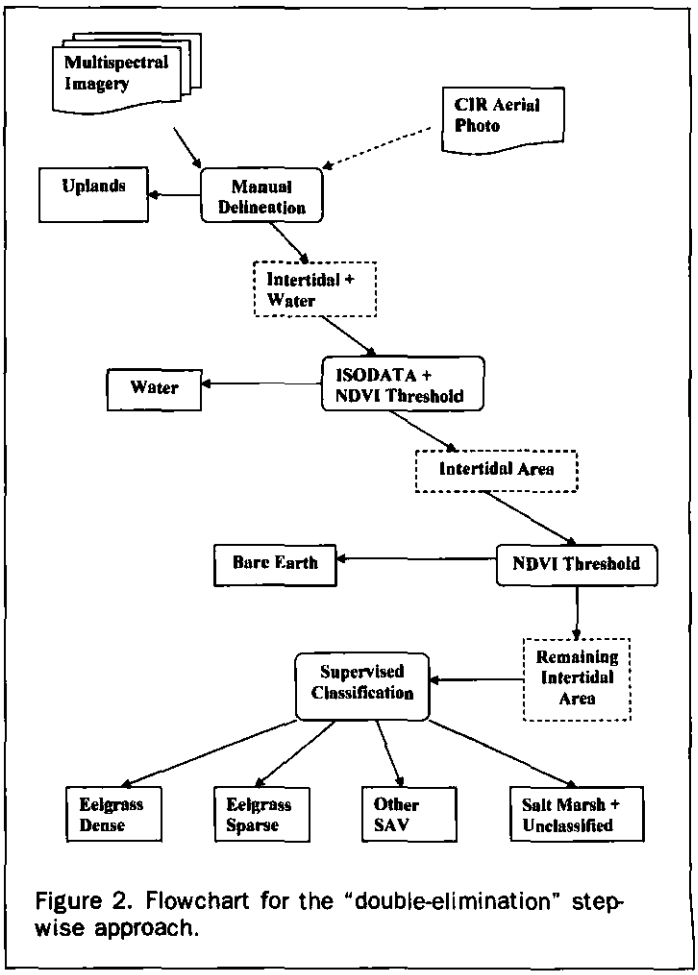

Figure 2. Flowchart for the "double-elimination" stepwise approach.

Accuracy Analysis

We choose a photointerpretation approach rather than a field survey method to verify the image classification. This is largely because of cost and time constraints and the limitation of a narrow maximum low tide time window for a field validation.

We first used a stratified random point sampling approach to generate 295 points over the classified image. A minimum of 30 points was selected for each class to guarantee a 90 percent confidence interval for accuracy, as suggested by Congalton (1991) and others (Senseman *et al.*, 1995; Jensen, 1986; Fitzpatrick-Lins, 1981; van Genderen and Lock, 1977). After generating 295 points, we used each point to define the center of a 2 × 2 pixel window. The window size of 10 × 10 m (5 m per pixel) was chosen mainly because the geometric accuracy of the scanner data was estimated at ±5 m.

We overlaid 295 accuracy point windows on the classified image to extract class value for each point with a majority rule within the 10 × 10 m area (or the 2 × 2 pixel window). The field survey personnel and other experts with extensive wetland experience independently conducted the photointerpretation of each accuracy point window overlaid on the DOQ base map (2 m pixel resolution). The CIR photographs (1-foot resolution) of the study area also were used to assist the interpretation process for verification of each class. The vegetation of each 10 × 10 m area was interpreted and classified based on the proportion of the area covered by each class and a visible estimate of eelgrass area.

The area coverage by the DOQ was smaller than the total area of the airborne scanner classified image. Therefore,

only 260 of 295 accuracy point windows were clearly identifiable on the DOQ base map layer. The remaining 35 accuracy point windows were either outside of the DOQ area coverage or within tree shadow areas. So, we excluded them in the final accuracy assessment.

Results and Discussion

Mapping Accuracy Evaluation

The final confusion matrix for the overall accuracy assessment is shown in Table 4. We archived an overall accuracy of 92 percent for mapping eelgrass in this study with 0.92 Kappa Coefficient. We must point out that we obtained the overall accuracy of 92 percent after lumping unclassified (2.8 percent) pixels into the "salt marsh" class as "salt marsh/mixed." Two of the 34 point areas photointerpreted as the eelgrass sparse class were misclassified as the bare earth class; while 3 of the 34 point areas photointerpreted as the eelgrass sparse class were categorized as the eelgrass dense (Table 4). We believe that the brightness of the sediments, the difference in spatial resolution between the scanner image and the DOQ CIR aerial photographs, and possible georeferencing accuracy may have caused the uncertainty of boundaries among these three classes.

We further evaluated producer and user accuracy for each individual class and found that the producer accuracy for eelgrass sparse (76.5 percent) and user accuracy for other SAV (77.1 percent) were relatively low (Table 5). Some uncertainty between eelgrass and other SAV may exist because of spectral (mostly mixing of background brightness) and spatial limitations in the data and in the classification procedures. However, a 95 percent of producer accuracy for "eelgrass dense" class was impressive for eelgrass mapping. The results seem to be in agreement with the early study carried out by Ritter and Lanzer (1997) in the same region with a CASI scanner. In addition, Mumby and Edwards (2002) concluded an 89 percent of overall accuracy over a coarse habitat area (including coral, macroalgae, seagrass, and sand habitats) in the Turks and Caicos Islands of British West Indies using a similar CASI scanner. They also compared the CASI sensor with Landsat TM and Ikonos satellite sensors, which yielded an overall accuracy of 73 percent and 68 percent, respectively. Ferguson and Korfmacher (1997) reported a similar overall accuracy of 72.6 percent for Landsat TM in their study carried in the coastal region of North Carolina. Results from previous studies and this study suggest that the advantage of spectral and spatial resolution of multispectral scanners can play an important part for eelgrass mapping. Despite of some confusing within eelgrass classes (dense and sparse), results from this study indicate that the use of airborne multispectral scanner data for eelgrass mapping can be practical and useful even though there may be some room for further improvement by refining and developing a more accurate, cost saving, and efficient procedure.

Implementation for Coastal Ecosystem Mapping

Eelgrass, *Zostera marina*, is one of the best-understood marine benthic plants, both in terms of life history and as a bioindicator (Berry *et al.*, 2003). Therefore, monitoring the health of eelgrass beds is an indirect measure of the many ecological functions performed by these biologically rich areas. Natural fluctuations in eelgrass abundance are important to understand in order to accurately access human-induced changes and to prevent or minimize them in the future. Our high-resolution survey accurately mapped the intertidal eelgrass beds as they occurred in July 2000. Most of the subtidal beds were also mapped as the leaves of plants in this area were floating on the surface during the approximately −0.9 m (−3 feet) MLLW tide that occurred in our study area on 30 July 2000. Dive surveys in the Similk Bay conducted in a previous study (Washington Department of Natural Resources, 1996) found that the eelgrass beds only extended down to a water depth of approximately −1.5 m (5 feet) MLLW. By surface inspections of the Skagit Bay beds in this study, we found that most of the beds were much shallower than the maximum depth (−8.8 m or −29 feet MLLW) reported by Berry *et al.* (2003) for eelgrass beds in Puget Sound. Future surveys using a similar remote sensing technology at a water depth of near MLLW should give a clear indication of the changes, if any, in eelgrass distribution and abundance. If significant changes have occurred, further investigations would be needed to evaluate those chemical and physical stressors that may be responsible for those changes.

Tribal, state, and federal agencies are vitally interested in the health of shoreline resources that support many fish and invertebrate species of subsistence, recreational, or commercial value. An example of these concerns is the Washington Department of Fish and Wildlife policy of "no-net-loss" of eelgrass beds (Fresh, 1994). Intergovernmental coordination and actions would likely be required in the event that the distribution and abundance of eelgrass beds in our study area were significantly reduced. The present eelgrass survey would serve as the baseline from which changes could be assessed.

Conclusion and Remarks

This study has demonstrated that high-resolution airborne multispectral scanner data can be valuable and useful for mapping eelgrass beds at local and regional scales. The overall accuracy of 92 percent using the airborne multispectral scanner in this study seems to agree with previous studies carried out in the same region (Strittholt and Frost, 1996; Ritter and Lanzer, 1997) and other locations (Bajjouk *et al.*, 1996; Mumby *et al.*, 1997; Mumby and Edwards,

TABLE 4. CONFUSION MATRIX FOR THE OVERALL ACCURACY ASSESSMENT WITH THE 260 POINT LOCATIONS

Class \ Grd Truth	Eelgrass Sparse	Bare Earth	Eelgrass Dense	Other SAV	Salt Marsh/Mixed	Total
Eelgrass sparse	**26 (76.5%)**[1]	2	2	0	0	30
Bare Earth	2	**83 (92.2%)**	0	0	0	85
Eelgrass dense	3	2	**75 (94.9%)**	0	1	81
Other SAV	3	3	2	**27 (100%)**	0	35
Salt marsh/mixed	0	0	0	0	**29 (96.7%)**	29
Total	34	90	79	27	30	**260**

Overall accuracy = 92.3%, Kappa Coefficient 0.92

Note: [1]indicates that the producer accuracies in the parentheses.

TABLE 5. PRODUCER AND USER ACCURACY ASSESSMENT

Class	Commission (%)	Omission (%)	Producer Accuracy (%)	User Accuracy (%)
Eelgrass sparse	15.4	30.8	76.5	86.7
Bare earth	2.4	8.4	92.2	97.6
Eelgrass dense	8	5.3	94.9	92.6
Other SAV	29.6	0	100	77.1
Salt marsh/mixed	0	3.4	96.7	100

2002). An excellent producer accuracy of 95 percent was obtained for eelgrass dense class. The relatively low producer accuracy of 76.5 percent for eelgrass sparse class needs to be further improved. Some uncertainty of mixing spectral response between eelgrass sparse and other SAV may be related to the variation of sediment background brightness, spectral and spatial resolution of the imagery. Development of improved classification procedures and a better sensor technology, such as hyperspectral scanners, may be further studied specifically for eelgrass mapping.

Some technical advantages of using the airborne multispectral scanner can be summarized as: (a) flexible acquisition time that can be scheduled at or near maximum low-tide time windows to reduce water column effect and to minimize cloud cover; (b) relatively high spatial and spectral resolution for local scale mapping; and (c) the use of more automated image classification procedures rather than the time-consuming field survey approach.

We also suggest that acquisition of airborne multispectral scanner imagery at and near maximum low tide time windows can optimize the detection and delineation of eelgrass beds in relatively deeper water.

Acknowledgments

This study was partly funded by the NASA Earth Science Applications Division (Contract No: NAS2-03144) as a joint NASA-EPA effort to demonstrate advanced monitoring technology to protect the environment. The work was also part of a larger technical assistance effort provided by the U.S. EPA, Region 10, for the Swinomish Indian Tribal Community (SITC). Administrative support for the project was provided by R. Parkin and P. Cirone. Field support for baseline surveys during the time of the over flight was provided by R. Clark, M. Gubitosa, L. Herger, K. Mendelman, A. Smith, E. Somers, D. Terpening, D. Thompson, and T. Reichgott from EPA Region 10 and A. Noffke from the SITC. P. Clinton and D. Young from EPA's ORD Laboratory in Newport, Oregon provided valuable input on the design and implementation of the field surveys. The over flight operation was provided by the U.S. DOE Remote Sensing Laboratory (RSL) in Las Vegas, Nevada. We would like to thank Tim McCreary (mission manager), Jim Newhouse (pilot), Dallin Wrigley (copilot), Marc Rivera (camera operator), Vic Young (sensor operator) and other flight operation personnel for their field support. Beth Vairin, editor of the USGS National Wetlands Research Center, helped our first draft manuscript editing. Valuable comments and suggestions to our original manuscript from three anonymous reviewers are also greatly appreciated.

References

Bajjouk, T., B. Guilaumont, and J. Populus, 1996. Application of airborne imaging spectrometry system data to intertidal seaweed classification and mapping, *Hydrobiologia*, 327:463–471.

Bajjouk, T., J. Populus, and B. Guilaumont, 1998. Quantification of subpixel cover fractions using principal component analysis and a linear programming method: Application to the coastal zone of Roscoff (France), *Remote Sensing of Environment*, 64:153–165.

Berry, H.D., A.T. Sewell, S. Wyllie-Echeverria, B.R. Reeves, T.F. Mumford, Jr., J.R. Skalaski, R.C. Zimmerman, and J. Archer, 2003. *Puget Sound Submerged Vegetation Monitoring Project: 2000–2002 Monitoring Report*, Nearshore Habitat Program, Washington State Department of Natural Resources, Olympia, Washington, 60 p. with appendices.

Congalton, R.G., 1991. A review of assessing the accuracy of classifications of remotely sensed data, *Remote Sensing of Environment*, 37:35–46.

Dennison, W.C., R.J. Orth, K.A. Moore, J.C. Stevenson, V. Carter, P.W. Bergstrom, and R.A. Batiuk, 1993. Assessing water quality with submerged aquatic vegetation: habitat requirements as barometers of Chesapeake Bay health, *Bio Science*, 43(2): 86–94.

Dobson, J.E., E.A. Bright, R.L. Ferguson, D.W. Field, L.L. Wood, K.D. Haddad, H. Iredale III, J.R. Jensen, V.V. Klemas, R.J. Orth, and J.P. Thomas, 1999. *NOAA Coastal Change Analysis Program (C-CAP) – Guidance for Regional Implementation*, NOAA Technical Report NMFS 123, Department of Commerce, April 1995, Revised, November 1999.

Ferguson, R.L., and K. Korfmacher, 1997. Remote sensing and GIS analysis of seagrass meadows in North Carolina, USA, *Aquatic Botany*, 58:241–258.

Ferguson, R.L., and L.L. Wood, 1990. Mapping submerged aquatic vegetation in North Carolina with conventional aerial photography, *Federal Coastal Wetland Mapping Programs*, (S.J. Kiraly, F.A. Cross, and J.D. Buffington, editors), pp. 125–133. U.S. Fish and Wildlife Service Biological Report, 90(18).

Ferguson, R.L., L.L. Wood, and D.B. Graham, 1993. Monitoring spatial change in seagrass habitat with aerial photography, *Photogrammetric Engineering & Remote Sensing*, 56: 597–603.

Fizpatrick-Lins, K., 1981. Comparison of sampling procedures and data analysis for a land-use and land-cover map, *Photogrammetric Engineering & Remote Sensing*, 47(3):343–366.

Fresh, K.L., 1994. Seagrass management in Washington State Wyllie-Echeverria, S., A.M. Olson, and M.J. Hershman, editors, *Seagrass Science and Policy in the Pacific Northwest: Proceedings of a Seminar Series*, (SMA 94–1), EPA 910/R-94-004, pp. 38–41.

Handley, L.R., A. Calix, and K. Mouton, 2004. Status and trends of seagrass of the Northern Gulf of Mexico (Abstract), *Presentation of 2004 Annual Meeting of Association of American Geographers (AAG)*, Philadelphia, 14–19 March.

Jensen, J.R., 1986. *Introductory Digital Image Processing*, Prentice-Hall, Englewood Cliffs, New Jersey, 227 p.

Moore, K.A., H.A. Neckles, and R.J. Orth, 1996. *Zostera marina* (eelgrass) growth and survival along a gradient of nutrients and turbidity in the lower Chesapeake Bay, *Marine Ecology Progress Series*, 142:247–259.

Mumby, P.J., E.P. Green, A.J. Edwards, and C.D. Clark, 1997. Measurement of seagrass standing crop using satellite and digital airborne remote sensing, *Marine Ecology Progress Series*, 159:51–60.

Mumby, P.J., E.P. Green, A.J. Edwards, and C.D. Clark, 1999. The cost-effectiveness of remote sensing for tropical coastal resources assessment and management, *Environmental Management*, 55:157–166.

Mumby, P.J., and A.J. Edwards, 2002. Mapping marine environments with IKONOS imagery: enhanced spatial resolution can deliver greater thematic accuracy, *Remote Sensing of Environment*, 82:248–257.

Lubin, D., W. Li, P. Dustan, C.H. Mazel, and K, Stamnes, 2001. Spectral signatures of coral reefs: features from space, *Remote Sensing of Environment*, 75:127–137.

Pasqualini, V., C. Pergent-Martini, P. Clabaut, H. Marteel, and G. Pergent, 2001. Integration of aerial remote sensing, photogrammetry, and GIS technologies in seagrass mapping, *Photogrammetric Engineering & Remote Sensing*, 67:99–105.

Phillips, R.C., 1972. *Ecological Life History of Zostera marina. (Eelgrass) in Puget Sound, Washington*, Ph.D. Dissertation, University of Washington, Seattle, 154 p.

Ritter, R., and E.L. Lanzer, 1997. Remote sensing of nearshore vegetation in Washington State's Puget Sound, *Proceedings of 1997 Geospatial Conference*, Seattle, Washington, 3: 527–536.

Senseman, G.M., C.F. Bagley, S.A. Tweddale, 1995. *Accuracy Assessment of the Discrete Classification of Remotely Sensed Digital Data for Landcover Mapping*, USACERL Technical Report EN-95/04, April.

Short, F.T., and D.M. Burdick, 1996. Quantifying eelgrass habitat loss in relation to housing development and nitrogen loading in Waquoit Bay, Massachusetts, *Estuaries*, 19: 730–739.

Strittholt, J.R., and P.A. Frost, 1996. *Determining Abundance and Distribution of Eelgrass (Zostera spp.) in Tillamook Bay Estuary, Oregon using Multispectral Airborne Imagery*, Report Prepared for Tillamook Bay National Estuary Project, Under Cooperative Agreement #CE990292-1 with the U.S. Environmental Protection Agency, 19 p.

Tyler-Walters, H., 2004. Zostera marina. Common eelgrass, *Marine Life Information Network: Biology and Sensitivity Key Information Sub-programme*, Plymouth: Marine Biological Association of the United Kingdom, URL: http://www.marlin.ac.uk/ (last date accessed: 10 April 2006).

van Genderen, J.L., and B.F. Lock, 1977. Testing land-use map accuracy, *Photogrammetric Engineering & Remote Sensing*, 43(9):1135–1137.

Washington Department of Natural Resources, 1996. Puget Sound intertidal habitat inventory 1996, 7.5 minute habitat series, *Anacortes quadrangle*, Aquatic Resource Division, Nearshore Habitat Program, Olympia, Washington, 37 p.

Young, D.R., D.T. Specht, P.J. Clinton, and H. Lee II, 1998. Use of color infrared aerial photography to map distribution of eelgrass and green macroalgae in a non-urbanized estuary of the Pacific Northwest U.S.A., *Proceedings of the Fifth International Conference on Remote Sensing for Marine and Coastal Environments*, Vol. II, Ann Arbor, Michigan, pp. 37–45.

(Received 06 January 2005; accepted 22 April 2005; revised 11 May 2005)